NUMERICAL STUDY OF THE SUPERADIABATIC FLAME TEMPERATURE PHENOMENON IN HYDROCARBON PREMIXED FLAMES

FENGSHAN LIU,[1] HONGSHENG GUO,[1] GREGORY J. SMALLWOOD[1] AND ÖMER L. GÜLDER[2]

[1]*Combustion Technology Group*
Institute for Chemical Process & Environmental Technology
National Research Council Canada
Building M-9, 1200 Montreal Road
Ottawa, Ontario, Canada K1A 0R6
[2]*University of Toronto*
Institute for Aerospace Studies
4925 Dufferin Street
Toronto, Ontario, Canada M3H 5T6

The phenomenon of superadiabatic flame temperature that was numerically predicted and experimentally observed in rich acetylene/oxygen flames used in chemical vapor deposition of diamond layers is of fundamental interest to combustion science. The chemical mechanism of this phenomenon has not been systematically studied. In this paper, the structure of planar freely propagating premixed flames of mixtures of CH_4/air, CH_4/O_2, C_2H_2/H_2/O_2, C_2H_4/O_2, C_3H_8/O_2, and H_2/O_2 was computed using detailed chemistry and complex thermal and transport properties to gain an insight into the common chemical mechanism responsible for this phenomenon in these flames. It was found that superadiabatic temperatures occur only in hydrocarbon flames when the equivalence ratio of the mixture is greater than a critical value, but not in hydrogen flames. The superadiabatic temperature in these hydrocarbon flames is associated with superequilibrium concentrations of some hydrocarbon species and H_2O, and with negative heat production rates at the end of main heat release reactions. The net negative heat production is caused by the endothermic dissociation reactions of these superequilibrium larger hydrocarbon molecules into smaller ones and of H_2O into H_2 and OH. In hydrogen flames, neither the concentration of H_2O nor the flame temperature exceeds their superequilibrium level. Radiation heat loss has negligible effect on the peak flame temperature and therefore does not affect the occurrence or the degree of superadiabatic temperatures.

Introduction

Study of the structure of laminar premixed hydrocarbon flames is of fundamental research interest in combustion science and is also a necessary first step toward understanding of turbulent premixed flames of practical interest. Detailed modeling of laminar premixed flames also plays an important role in developing turbulent combustion models within the framework of the flamelet model. It is also important to help understand the experimental results obtained in rich premixed hydrocarbon flames used for chemical vapor deposition (CVD) of diamond thin film to meet the requirements of fast and hot flames that can deliver a large flux of H radical to the substrate [1–4].

The structure of laminar premixed flames has been studied numerically previously by many researchers, for example, Refs. [5–7]. However, in these studies attention was primarily paid to the structure of lean, stoichiometric, or slightly rich premixed flames where superadiabatic flame temperatures do not occur. In a numerical study of diamond CVD using a strained rich premixed C_2H_2/H_2/O_2 flame, Meeks et al. [8] found that the flame temperature exceeds the adiabatic temperature, which is somewhat unusual in premixed hydrocarbon flames. Their study is perhaps the first numerical work to reveal the phenomenon of superadiabatic temperature in rich premixed hydrocarbon flames. The appearance of superadiabatic temperature in the flame numerically studied by Meeks et al [8] was subsequently confirmed experimentally by Bertagnolli and Lucht [3] and Bertagnolli et al. [4]. Meeks et al. [8] suggested that the primary reason for the occurrence of the superadiabatic flame temperatures in the rich C_2H_2/H_2/O_2 premixed flame is that unreacted acetylene requires a relatively long time to dissociate to its equilibrium concentration. The slow and endothermic dissociation of acetylene was believed to be responsible for the superequilibrium concentrations of acetylene and superadiabatic flame temperatures. Another explanation of the superadiabatic flame temperatures in this flame was later presented by Bertagnolli et al. [4], who believed that the presence of superequilibrium concentrations of CO_2 and H_2O is the primary cause of
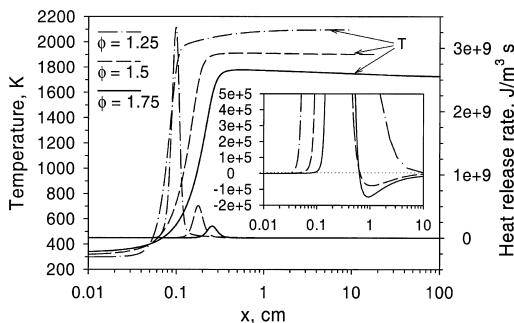
FIG. 1. Distributions of temperature and heat-release rate in the three CH_4/air flames. The inset is an enlarged version of, the heat-release rate around 0 to show the occurrence of negative values.

the superadiabatic flame temperatures. The super-equilibrium concentrations of C_2H_2 and H_2O are consistent with the subequilibrium concentrations of H and H_2. More recently, in a numerical study of CVD of diamond films using rich acetylene-oxygen flames, Ruf et al. [9] also noticed the significantly subequilibrium concentration of H and suggested that the slow and endothermic reaction $H_2 + M \Leftrightarrow H + H + M$ is responsible for the subequilibrium concentration of H and superadiabatic flame temperatures. While the superadiabatic flame temperature phenomenon is clearly a non-equilibrium process, this brief review of the literature on this topic reveals that our current understanding of the chemical mechanism for this phenomenon is incomplete and more studies of the associated reaction pathways and chemical mechanism are required. In contrast, more research has been devoted to the mechanism of superadiabatic temperature in diffusion flames, such as the numerical study of Takagi and Xu [10]. It is generally believed that the superadiabatic temperatures in diffusion flames are a direct consequence of the preferential diffusion effects of H_2 and H.

In the present study, the structure of several atmospheric freely propagating planar premixed flames in mixtures of CH_4/air, CH_4/O_2, $C_2H_2/H_2/O_2$, C_2H_4/O_2, C_3H_8/O_2, and H_2/O_2 was numerically computed using detailed chemistry and complex thermal and transport properties. The objectives of this study are (1) to ascertain if the superadiabatic flame temperature is a common phenomenon in rich hydrocarbon premixed flames or a phenomenon that only occurs in certain flames, (2) to identify the reaction pathways responsible for the superadiabatic flame temperature and determine whether a common mechanism for superadiabatic flame temperature exists when it occurs, and (3) to investigate the effects of radiation heat loss on the occurrence of the superadiabatic flame temperature.

Numerical Model

The conservation equations of mass, energy, and chemical species for steady planar freely propagating premixed flames were solved using a CHEMKIN-based code [11]. The thermochemical and transport properties of species were obtained from CHEM-KIN [11] and TPLIB [12,13] database. Most of the calculations were conducted without radiation heat loss in order to highlight the effect of chemical kinetics. However, two runs with radiation heat loss were conducted in order to assess its effect on the occurrence of superadiabatic flame temperature. At a spatial location of $x = 0.05$ cm, the mixture temperature is fixed at 400 K. In all the calculations, the upstream location (fresh mixture) is always kept at $x = -2.5$ cm. The location of downstream (reacted combustion products) specified in the calculations varies with the gas mixture. In all the calculations, however, it was checked that the computational domain was sufficiently long to achieve adiabatic equilibrium when radiation heat loss was not included. The gas mixture temperature at the upstream boundary was kept at 298 K, and zero-gradient conditions were specified at the downstream boundary. All the calculations were performed at atmospheric pressure. The GRI Mech 3.0 reaction mechanism [14] was used to model the chemical kinetics in all the hydrocarbon flames considered in this work. The only modification made to this mechanism is the removal of species and reactions related to NO_x formation. This reaction mechanism was primarily developed for natural gas combustion and therefore may not be an optimized reaction mechanism for acetylene, ethylene, and propane flames. However, it is believed that use of the GRI mechanism is still adequate for these flames investigated here since the heat-release rate is of primary interest in the present context as far as the superadiabatic flame temperature is concerned. The reaction mechanism used in the calculations of the hydrogen flame is that used previously by Smooke et al. [15].

Results and Discussions

Methane/Air Flames

Three planar freely propagating methane/air flames were computed. The equivalence ratios (ϕ) of these flames are 1.25, 1.5, and 1.75. Fig. 1 shows the temperature and heat-release rate distributions in these three flames. Superadiabatic flame temperature occurs for the two richer flames, that is, $\phi = 1.5$ and 1.75, but not for the flame of $\phi = 1.25$. The peak temperature in the richest methane/air flame of $\phi = 1.75$ is higher than the adiabatic flame temperature by about 50 K. The occurrence of superadiabatic temperature is associated with negative
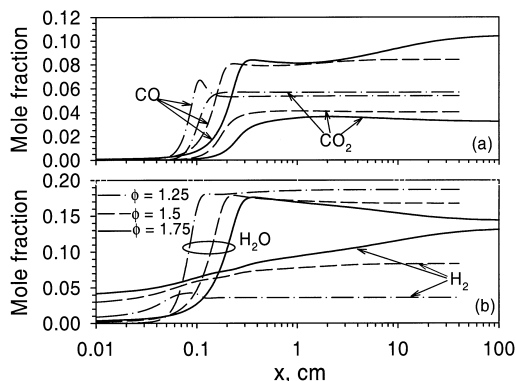
FIG. 2. Distributions of mole fraction of CO, CO_2, H_2, and H_2O in the three CH_4/air flames.
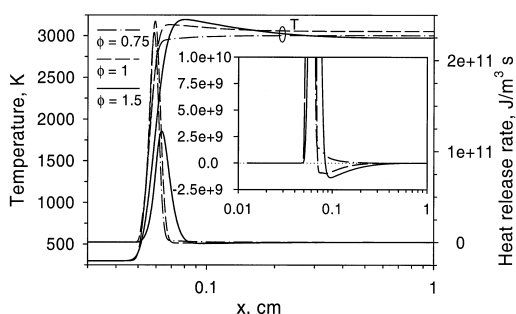
FIG. 3. Distributions of temperature and heat-release rate in the three CH_4/O_2 flames. The inset is an enlarged version of the heat-release rate around 0 to show the occurrence of negative values.

heat-release rates in the immediate postflame region, shown in detail in the inset of Fig. 1. The mole fraction distributions of four important species CO, CO_2, H_2, and H_2O are shown in Fig. 2 for these flames. As the equivalence ratio increases, the concentrations of the intermediate species CO, H_2, and other hydrocarbon species (not shown) in the final products increase, while the concentrations of stable species CO_2 and H_2O decrease. For $\phi = 1.25$, where the flame temperature does not exceed the adiabatic equilibrium value, both CO_2 and H_2O remain subequilibrium at the end of the major heat-release reactions (approximately at $x = 0.1$ cm) and then gradually approach their equilibrium levels. However, CO and H_2 become superequilibrium at around $x = 0.1$ cm then drop rapidly to their equilibrium concentrations. The primary pathways for the conversion of CO to CO_2 and H_2 to H_2O are CO $+$ OH $\Rightarrow CO_2 +$ H and $H_2 +$ OH $\Rightarrow H_2O +$ H. In the two richer flames of $\phi = 1.5$ and 1.75, the scenario is completely different. The peak mole fractions of CO_2 in these two flames are slightly higher than the corresponding equilibrium levels, while the

mole fractions of H_2O are significantly superequilibrium, especially in the flame of $\phi = 1.75$. On the other hand, CO and H_2 in these two richer flames remain subequilibrium. The mole fractions of the three important free radicals OH, H, and O in the methane/air flames (not shown) significantly exceed their equilibrium concentrations in the reaction zone in all three flames.

As shown in the inset of Fig. 1, the heat-release rates for the two richer methane/air flames become negative at the end of the main heat-release reactions and then gradually recover to zero, that is, toward the adiabatic equilibrium state. A detailed analysis was conducted for the richest methane/air flame ($\phi = 1.75$) in order to identify the reaction pathways that are responsible for the endothermicity in the postflame region. It was found that the negative heat-release rate in the postflame region is primarily caused by the following slow and endothermic reactions: $CH_2CO +$ M $\Rightarrow CH_2 +$ CO $+$ M, $C_2H_5 +$ M $\Rightarrow$ H $+ C_2H_4 +$ M, $C_2H_3 +$ M $\Rightarrow$ H $+ C_2H_2 +$ M, H $+ H_2O \Rightarrow$ OH $+ H_2$. Endothermic dissociation reactions involving CH_2OH, C_2H_4, CH_3, HCO, and CO_2 also contribute to the endothermicity in the postflame region to a lesser degree. In addition, the endothermic chain-branching reaction H $+ O_2 \Rightarrow$ O $+$ OH contributes significantly to reduce the heat-release rate from positive to negative. Then it quickly reaches equilibrium at the location of the lowest value of the heat-release rate. The dissociation of CO_2 to CO and H_2O to H_2 in this flame ($\phi = 1.75$) in the postflame region is consistent with the superequilibrium concentrations of CO_2 and H_2O and the subequilibrium levels of CO and H_2 shown in Fig. 2.

The results of the three CH_4/air flames indicate that non-equilibrium prevails in the immediate post-region of major heat-release reactions due to insufficient residence time to reach equilibrium. Under usual conditions such as the flame of $\phi = 1.25$ where superadiabatic flame temperatures do not occur, the approach from non-equilibrium to equilibrium in the postflame region is through a series of slow and exothermic reactions. However, with increasing the equivalence ratio, the non-equilibrium state in the immediate postflame region is such that its approach to equilibrium involves a series of slow and endothermic reactions due to dissociation of superequilibrium hydrocarbon species and H_2O formed in the reaction zone. The formation of these superequilibrium species is responsible for superadiabatic temperatures.

Methane/Oxygen Flames

The structure of three CH_4/O_2 flames was computed, a lean flame of $\phi = 0.75$, a stoichiometric flame, and a rich flame of $\phi = 1.5$. Fig. 3 shows the temperature and heat-release rate distributions of
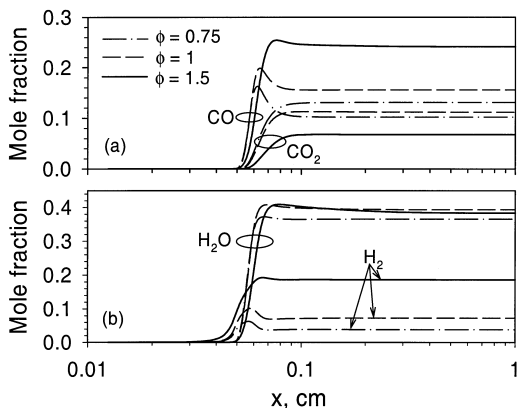
FIG. 4. Distributions of mole fraction of (a) CO, CO_2, (b) H_2, and H_2O in the three CH_4/O_2 flames.

these flames. The inset in this figure is an enlargement of the heat-release rate around zero. Superadiabatic flame temperatures occur in the stoichiometric and the rich flames, accompanied by the negative heat-release rates in the postflame regions in these two flames. Although the adiabatic temperature of the rich flame is lower than that of the stoichiometric one, the peak flame temperature in the rich flame is higher. The peak flame temperatures in these two flames exceed their respective adiabatic flame temperature by about 81 and 220 K. Mole fraction distributions of four species, CO, CO_2, H_2, and H_2O, are shown in Fig. 4. The peak concentration of the two intermediate species, CO and H_2, exceeds their adiabatic equilibrium levels in all three flames, although the degree of superequilibrium concentration decreases with increasing ϕ. The concentration of CO_2 in the postflame region is slightly subequilibrium in the lean flame and only slightly superequilibrium in the stoichiometric flame and the rich flame. The concentration of H_2O becomes superequilibrium in all three flames (Fig. 4) and the degree of superequilibrium increases with ϕ. Compared with the concentration distributions of these species in the methane/air flames shown in Fig. 2, it can be seen that CO_2 and H_2O profiles exhibit some similarity, but H_2 and CO profiles are rather different. Unlike the results for the methane/air flames where the concentrations of radicals O, H, and OH are substantially superequilibrium, the three radicals in the methane/oxygen flames remain either subequilibrium or only slightly superequilibrium. Only the H radical at the end of major heat-release reactions of the rich flame is significantly lower than its equilibrium concentration. This difference is perhaps caused by the close-to-equilibrium reactions involving these radicals at much higher temperatures in these methane/oxygen flames.

A detailed analysis of the heat production rate of all the reactions in the rich CH_4/O_2 flame was conducted in order to identify the reaction pathways leading to the endothermicity in the postflame region. The following reactions are found to be responsible for the endothermicity in the postflame region of the rich CH_4/O_2 flame: $H_2O + M \Rightarrow H + OH + M$, $H_2 + H_2O \Rightarrow 2H + H_2O$, $O_2 + H_2O \Rightarrow OH + HO_2$, $CO_2 + M \Rightarrow O + CO + M$, $HO_2 + H_2O \Rightarrow H + O_2 + H_2O$, $H_2 + M \Rightarrow 2H + M$, $O + H_2O \Rightarrow 2OH$, $HO_2 + H_2O \Rightarrow OH + H_2O_2$, $H_2O_2 + M \Rightarrow 2OH + M$, $H + H_2O \Rightarrow OH + H_2$. However, almost all the endothermicity in the postflame region is contributed by the first three reactions that reduce the superequilibrium concentration of H_2O to its equilibrium level. Similar to the richest CH_4/air flame discussed earlier, the endothermic chain-branching reaction $H + O_2 \Rightarrow O + OH$ also contributes significantly to reduce the heat-release rate from positive to negative. Again, it quickly reaches equilibrium at the location of the lowest value of the heat-release rate. It is interesting but not surprising to notice that the decay of CO_2 toward to equilibrium in this flame is through $CO_2 + M \Rightarrow O + CO + M$ rather than $H + CO_2 \Rightarrow OH + CO$, which is the reaction pathway in the CH_4/air flame of $\phi = 1.75$. It is also interesting to observe that the species involved in the postflame endothermic reactions are either hydrogen-oxy or carbon-oxy species, but not hydrocarbon species. In this regard, this flame is different from the CH_4/air flame of $\phi = 1.75$ where the endothermic reactions in the postflame region involve hydrocarbon species. Such a difference in the postflame reactions in the two rich CH_4/air and CH_4/O_2 flames can be explained as follows. In the rich CH_4/air flame of $\phi = 1.75$ where the flame temperatures remain lower than 1800 K, the temperature-sensitive dissociation reactions given at the end of the last section are much slower than those temperature-insensitive three-body recombination reactions. Therefore, the approach from non-equilibrium to equilibrium in the postflame region is through the slower hydrocarbon dissociation reactions. In contrast, in the rich CH_4/O_2 flame where the flame temperatures are about 3000 K, those temperature-sensitive dissociation reactions involving hydrocarbon species are believed to be more rapid than the temperature-insensitive three-body recombination reactions. Therefore, the three-body recombination reactions are the controlling reactions from non-equilibrium to equilibrium in the postflame region in the rich CH_4/O_2 flame.

The effect of radiation heat loss was investigated in the rich CH_4/O_2 flame. Numerical results show that the inclusion of the radiation sink term based on the optically thin approximation in the energy equation reduces the peak flame temperature by only less than 1 K. The temperature distribution
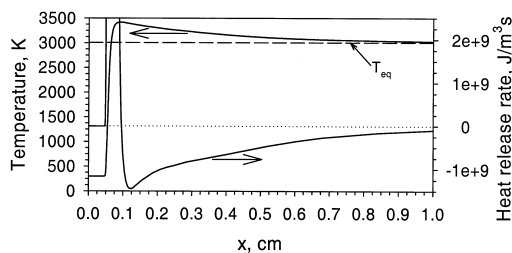
FIG. 5. Distributions of temperature and heat-release rate in the $C_2H_2/H_2/O_2$ flame.
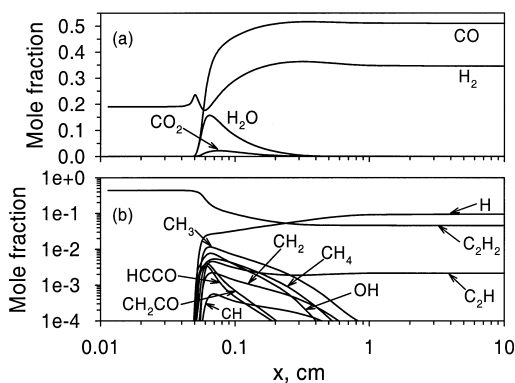
FIG. 6. Distributions of mole fraction of major species in the $C_2H_2/H_2/O_2$ flame.

with radiation heat loss is not shown in Fig. 3 since it is almost identical to the adiabatic one for $x < 1$ cm. However, the temperature in the non-adiabatic flame continues to drop with increasing distance, and at $x = 40$ cm, it is lower than the adiabatic temperature by about 70 K. It is therefore evident that, although radiation heat loss has a small impact, it does not affect the occurrence of the superadiabatic flame temperature.

Acetylene/Hydrogen/Oxygen Flame

The mole fractions of C_2H_2, H_2, and O_2 in the mixture of $C_2H_2/H_2/O_2$ are, respectively, 0.44, 0.19, and 0.37, the same as in the strained $C_2H_2/H_2/O_2$ flame previously numerically studied by Meeks et al. [8]. The temperature and heat-release distributions in this flame are shown in Fig. 5. The peak flame temperature is 3416.5 K, which is 410 K above the adiabatic flame temperature. The peak flame temperature in the strained flame of Meeks et al. [8] exceeds the adiabatic flame temperature by about 300 K, which is about 100 K lower than the peak flame temperature in the unstrained flame considered here, which is expected because of heat loss to the substrate in the strained flame of Meeks et al. This comparison of the peak flame temperatures in

the strained and unstrained $C_2H_2/H_2/O_2$ flame also provides some support for the use of the GRI Mech 3.0 mechanism in the computation of this flame for the purposes of the present study. Fig. 6 displays the mole fraction distributions of major species whose mole fractions are above 1×10^{-4}. It is interesting to see that there are only five major species, CO, H_2, H, C_2H_2, and C_2H, in the equilibrium composition. Concentrations of CO_2 and H_2O are significantly superequilibrium in the region between about $x = 0.05$ cm and $x = 0.3$ cm. Radiation heat loss was also found to have negligible effect on the peak temperature in this flame.

Analyses of the heat production rate of reactions in this flame revealed that the following reactions, in order of contribution, are primarily responsible for the endothermicity in the postflame region shown in Fig. 5: $C_2H_2 + M \Rightarrow H + C_2H + M$, $CH_4 + M \Rightarrow H + CH_3 + M$, $CH_2CO + M \Rightarrow CH_2 + CO + M$, $H_2O + H \Rightarrow OH + H_2$, $CH_3 + M \Rightarrow H + CH_2 + M$, $H_2 + M \Rightarrow 2H + M$, $2H_2 \Rightarrow 2H + H_2$, $HCCO + M \Rightarrow CH + CO + M$, $CH_3 + M \Rightarrow CH + H_2 + M$, $C_2H_3 + M \Rightarrow H + C_2H_2 + M$, $HCO + H \Rightarrow H_2 + CO$, $CO_2 + H \Rightarrow OH + CO$. At this point, it is interesting to note that the possible causes of the superadiabatic flame temperatures in this flame and in the C_2H_2/O_2 flame of Ruf et al. [9] speculated previously by Meeks et al. [8], Bertagnolli et al. [4], and Ruf et al. [9] are all relevant but are all incomplete in view of the results presented above. The present analysis indicates that the degree of temperature overshoot in the $C_2H_2/H_2/O_2$ flame is largely determined by the degree of concentration overshoot of C_2H_2, CH_4, CH_2CO, and H_2O.

Ethylene/Oxygen Flame

The structure of a rich C_2H_4/O_2 premixed flame of $\phi = 2$ was computed. Distributions of temperature, heat-release rate, and some species are shown in Figs. 7 and 8, respectively. Superadiabatic flame temperatures occur again in this flame and the peak flame temperature exceeds the adiabatic equilibrium temperature by about 388 K. The approach from non-equilibrium at the immediate postflame region
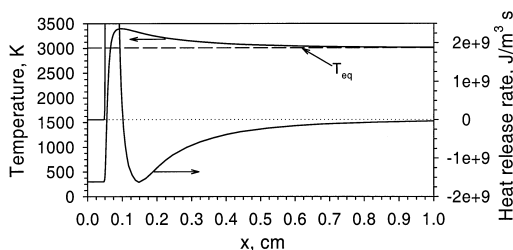
FIG. 7. Distributions of temperature and heat-release rate in the C_2H_4/O_2 flame.
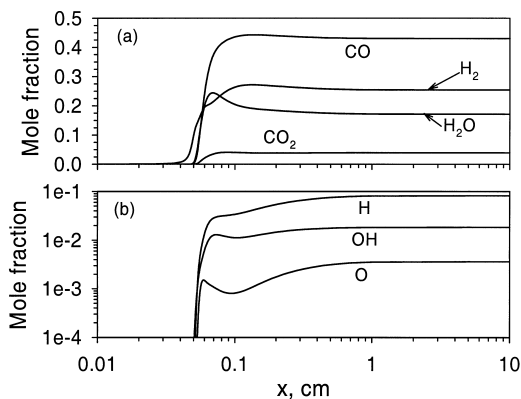
FIG. 8. Distributions of mole fraction of CO, CO_2, H_2, H_2O, O, H, and OH in the C_2H_4/O_2 flame.
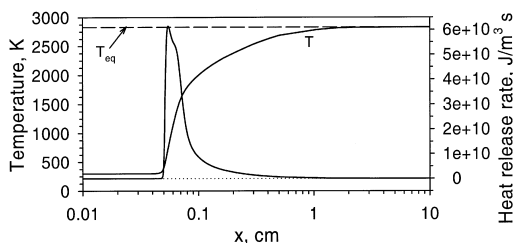
FIG. 9. Distributions of temperature and heat-release rate in the H_2/O_2 flame.
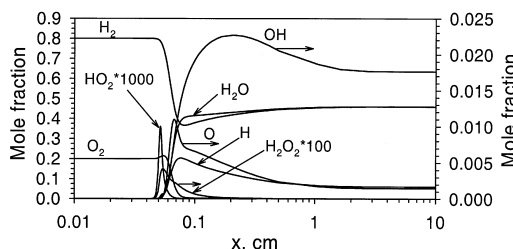
FIG. 10. Distributions of mole fraction of species in the H_2/O_2 flame.

to equilibrium is once again associated with negative heat-release reactions. In this flame, H_2O is significantly above its equilibrium level and H_2 is correspondingly below its equilibrium concentration (Fig. 8a). The peak CO mole fraction is only slightly above the equilibrium level and CO_2 is very close or to its equilibrium concentration around the location of peak temperature. Concentrations of the three important radicals O, H, and OH (Fig. 8b) remain subequilibrium in the reaction zone and in the postflame region.

The endothermicity in the postflame region in this flame was found to be primarily caused by the following reactions: $H_2O + M \Rightarrow H + OH + M$, H_2O

$+ H \Rightarrow OH + H_2$, $H_2 + H_2O \Rightarrow 2H + H_2O$, $H_2 + M \Rightarrow 2H + M$, $H_2 + H_2 \Rightarrow 2H + H_2$, $H + HCO \Rightarrow H_2 + CO$. While third-body decomposition reactions $CH_4 + M \Rightarrow H + CH_3 + M$, $CH_2CO + M \Rightarrow CH_2 + CO + M$, $HCCO + M \Rightarrow CH + CO + M$, $HCO + M \Rightarrow H + CO + M$, and $HCO + H_2O \Rightarrow H + CO + H_2O$ also contribute significantly to the transition of the heat-release rate from positive to negative, they reach equilibrium shortly after the heat-release rate becomes negative.

Propane/Oxygen Flame

The last hydrocarbon flame investigated is a rich C_3H_8/O_2 flame of $\phi = 2$. The structure of this flame is qualitatively similar to that of the C_2H_4/O_2 flame shown in Figs. 7 and 8. Although superadiabatic flame temperatures occur again in this flame, the degree of temperature overshoot is only about 154 K, much lower than that in the $C_2H_2/H_2/O_2$ and C_2H_4/O_2 flames discussed earlier. The slow and endothermic reactions in the postflame region consist of almost all the reactions identified in the C_2H_4/O_2 flame except reaction $H + HCO \Rightarrow H_2 + CO$, which are the pathways for H_2 and H_2O to approach from non-equilibrium to equilibrium. The decomposition of CH_4 and CH_2CO through $CH_4 + M \Rightarrow H + CH_3 + M$ and $CH_2CO + M \Rightarrow CH_2 + CO + M$ contribute significantly to the transition of the heat-release rate from positive to negative. The degree of temperature overshoot in this flame is primarily controlled by the levels of concentration overshoot of H_2O, CH_4, and CH_2CO.

Hydrogen/Oxygen Flame

The final flame considered in this study is a rich H_2/O_2 premixed flame with an equivalence ratio of 2. The computed profiles of temperature and heat-release rate and species mole fraction are shown in Figs. 9 and 10. These results indicate that the flame temperature in this rich hydrogen/oxygen flame does not exceed the adiabatic flame temperature, as also manifested by the fact that the heat-release rate stays positive, that is, the approach from non-equilibrium in the immediate postflame region to equilibrium is through some slow but exothermic reactions. The almost identical mole fractions of H_2 and H_2O at equilibrium in this flame shown in Fig. 10 are purely a coincidence. A detailed analysis of heat production rate of all the reactions reveals that the following three reactions are involved in the postflame region from non-equilibrium to equilibrium: $H + OH + M \Rightarrow H_2O + M$ (exothermic), $H + H + M \Rightarrow H_2 + M$ (exothermic), $H_2O + H \Rightarrow OH + H_2$ (endothermic). Results obtained at other equivalence ratios or for rich hydrogen/air flames

also confirm that superadiabatic flame temperatures do not occur in hydrogen flames.

A question raised from the qualitatively different behavior of flame temperature in the hydrocarbon and hydrogen flames is why the temperature of hydrogen flames never becomes superadiabatic. The answer to this question perhaps lies in the inhibiting effect of hydrocarbon species to the H_2-O_2 system as discussed by Westbrook and Dryer [16]. The inhibiting effect of hydrocarbon species is to compete effectively with the most important endothermic chain branching reaction $H + O_2 \Leftrightarrow O + OH$ through some relatively temperature-independent exothermic reactions such as $H + CH_2 + M \Rightarrow CH_3 + M$, $H + CH_3 + M \Rightarrow CH_4 + M$, and $H + HCO + M \Rightarrow CH_2O + M$. As a result, the concentrations of some stable hydrocarbon species, such as CH_4, CH_2CO, and H_2O, in these relatively rich hydrocarbon flames become superequilibrium near the end of major heat-release reactions. This is accompanied by superadiabatic flame temperatures. The subsequent endothermic dissociation reactions of these superequilibrium species bring their concentrations and the temperature back to the equilibrium levels.

Conclusions

A systematic study of the phenomenon of superadiabatic flame temperature in premixed flames was conducted by numerically computing the flame structure in mixtures of CH_4/air, CH_4/O_2, C_2H_2/H_2/O_2, C_2H_4/O_2, C_3H_8/O_2, and H_2/O_2 using detailed reaction mechanism and complex thermal and transport properties. Superadiabatic flame temperatures occur only in hydrocarbon premixed flames when the equivalence ratio reaches a critical value, but not in hydrogen flames. The occurrence of superadiabatic flame temperatures in hydrocarbon flames is caused by superequilibrium concentrations of some hydrocarbon species and H_2O. Radiation heat loss does not affect the occurrence or

the degree of temperature overshoot. The results of the present study show that the mechanism of superadiabatic flame temperatures in hydrocarbon flames is chemical kinetics.

REFERENCES

1. Murayama, M., Kojima, S., and Uchida, K., *J. Appl. Phys.* 69:7924 (1991).
2. Glumac, N. G., and Goodwin, D. G., *Combust. Flame* 105:321 (1996).
3. Bertagnolli, K. E., and Lucht, R. P., *Proc. Combust. Inst.* 26:1825 (1996).
4. Bertagnolli, K. E., Lucht, R. P., and Bui-Pham, M. N., *J. Appl. Phys.* 83:2315 (1998).
5. Tsatsaronis, G., *Combust. Flame* 33:217 (1978).
6. Smooke, M. D., *J. Comput. Phys.* 48:72–105 (1982).
7. Dixon-Lewis, G., *Proc. Combust. Inst.* 23:305 (1990).
8. Meeks, E., Kee, R. J., Dandy, D. S., and Coltrin, M. E., *Combust. Flame* 92:144 (1993).
9. Ruf, B., Behrendt, F., Deutschmann, O., Kleditzsch, S., and Warnatz, J., *Proc. Combust. Inst.* 28:1455 (2000).
10. Takagi, T., and Xu, Z., *Combust. Flame* 96:50 (1994).
11. Kee, R. J., Grcar, J. F., Smooke, M. D., and Miller, J. A., Sandia report SAND85-8240.
12. Kee, R. J., Miller, J. A., and Jefferson, T. H., Sandia report SAND 80-8003.
13. Warnatz, J., Kee, R. J., and Miller, J. A., Sandia report SAND 83-8209.
14. Smith, G. P., Golden, D. M., Frenklach, M., Moriarty, N. W., Eiteneer, B., Goldenberg, M., Bowman, C. T., Hanson, R. K., Song, S., Gardiner Jr., W. C., Lissianski, V. V., and Qin, Z., www.me.berkeley.edu/gri_mech/.
15. Smooke, M. D., Miller, J. A., and Kee. R. J., *Combust. Sci. Technol.* 34:79–90 (1983).
16. Westbrook, C. K., and Dryer, F. L., *Prog. Energy Combust. Sci.* 10:1–57 (1984).

COMMENTS

Burak Atakan, Gerhard-Mercator-University Duisburg, Germany. We investigated low pressure (50 mbar), diamond-forming acetylene/O/Ar flames and did not find any superadiabatic temperatures. Could you comment on the pressure dependence of the superadiabatic temperatures?

Author's Reply. We have numerically simulated the freely propagating C_2H_2/O_2/Ar flame at 50 mbar using CHEMKIN codes and the GRI-MECH 3.0 mechanism and found that the peak temperature is about 600 K above the adiabatic flame temperature. In fact, there are studies in the literature that reported superadiabatic temperatures

in rich C_2H_2 flames at low pressures [2,3]. In our view, the occurrence of superadiabatic temperatures in rich hydrocarbon flames is not pressure dependent. The explanation to your observation that superadiabatic temperatures did not occur in the experiment of [1] may lie in the fact that the cold gas velocity of 86 cm/s is believed to be much lower than the burning velocity of the mixture with R [O_2]/[C_2H_2] 1.4 based on our calculation. Under these conditions, use of an actively cooled (310 K) bronze porous plate caused the flame to be extinguished. Therefore, the chemical kinetics in the flame studied in [1] was complicated and therefore cannot even be qualitatively simulated using the freely propagating flame model.

REFERENCES

1. Löwe, A. G., Hartlieb, A. T., Brand, J., Atakan, B., and Kohse-Höinghaus, K., *Combust. Flame* 118:37 (1999).
2. Goodwin, D. G., Glumac, N. G., and Shin, H. S., *Proc. Combust. Inst.* 26:1817 (1996).
3. Ruf, B., Behrendt, F., Deutschmann, O., Kleditzsch, S., and Warnatz, J., *Proc. Combust. Inst.* 28:1455 (2000).

●

Mitchell D. Smooke, Yale University, USA. There is a body of work investigating superadiabatic flame temperatures in stretched premixed flames. In that work the Lewis number of the deficient reactant plays an important role. Have you considered Lewis number effects in helping to explain your results?

Author's Reply. Superadiabatic flame temperatures (SAFTs) occur in stretched premixed flames when the Lewis number is less than unity such as in hydrogen/air flames [1] and lean methane/air flames [2]. SAFT does not occur in stretched premixed flames when the mixture Lewis number is greater than unity. It is also important to note that the Lewis number effect weakens as the stretch rate decreases [1,3]. Since the present calculations were conducted in one-dimensional freely propagating premixed flames, it is expected that there is little or no help to explain the present results in terms of the Lewis number effect.

REFERENCES

1. Guo, H., Ju, Y., and Niioka, T., *Combust. Theory Modelling* 4:459 (2000).
2. Wang, J., and Niioka, T., *Proc. Combust. Inst.* 29:2211 (2002).
3. Ishizuka, S., and Law, C. K., *Proc. Combust. Inst.* 19:327 (1982).

●

Ishwar K. Puri, University of Illinois at Chicago, USA. While I applaud your inclusion of a radiation mode, namely, in the optically thin limit, I would hesitate to draw conclusions based on it for rich flames. Rich flames, as is well known, involve sooting and gas-phase radiation from species other than CO_2 and H_2O.

Author's Reply. Based on the critical sooting equivalence ratios (based on CO and H_2O as products) [1], the rich CH_4/O_2, C_2H_4/O_2, C_3H_8/O_2 flames studied in our paper are not sooting, while the $C_2H_2/H_2/O_2$ flame could be sooting. There are also other hydrocarbon species in rich flames that are radiatively active and therefore play some roles in radiation heat transfer. As quantitative information of soot concentration in the $C_2H_2/H_2/O_2$ flame and radiative properties of various hydrocarbon species is not available, contribution from soot and hydrocarbon species was not taken into account in the present calculations

employing the optically thin model. However, this does not alter the conclusion that radiation heat loss is unimportant in the occurrence of SAFT based on the maximum radiation loss estimation of Meeks et al. [2]. To estimate the maximum radiation loss effect on temperature in the $C_2H_2/H_2/O_2$ flame, Meeks et al. [2] compared the results of no radiation and of blackbody radiation (assuming gas mixture emissivity ($\varepsilon_g = 1$), and they found that the flame temperature is only lowered by less than 30 K in the postflame region.

REFERENCES

1. Glassman, I., *Combustion, 3rd ed.,* Academic Press, New York, 1996.
2. Meeks, E., Kee, R. J., Dandy, D. S., and Coltrin, M. E., *Combust. Flame* 92:144 (1993).

●

Paul Ronney, University of Southern California, USA. It is well known theoretically [1] and numerically [2] that radiative transport can lend to SAFTs even for one-step or lean mixtures with multistep chemistry when reabsorption effects are considered. This would be even more significant for rich mixtures because of the higher concentrations of radiatively participating species. Thus, experimentally observed SAFT could also be a result of radiation effects that were not considered in this work, since only optically thin radiative loss was modeled. Hydrogen-air mixtures have no radiatively participating species in the reactants, thus the reactants cannot absorb radiation emitted by the products. Consequently, it seems that other mechanisms could be responsible for experimentally observed SAFT.

REFERENCES

1. Joulin, G., and Peshaies, B., *Combust. Sci. Technol.* 47:299 (1986).
2. Ju, Y., Masuya, G., and Ronney, P. D., *Proc. Combust Inst.* 27:2619 (1998).

Author's Reply. It is true that the presence of radiating species in the fresh mixture of a premixed flame can give rise to SAFTs. It is also plausible that the experimentally observed SAFT could be a result of radiation absorption by hydrocarbon species in the unburned mixture. However, the fact that the numerically calculated level of SAFT in the $C_2H_2/H_2/O_2$ flame, in the absence of such mechanism, is close to that experimentally measured suggests that the degree of SAFT caused by radiation absorption effect is relatively unimportant in comparison to the chemical kinetics effect revealed in the present study. Both radiation and chemical kinetics effects favor the occurrence of SAFT in rich hydrocarbon flames. Our results indicate that chemical kinetics is the dominant mechanism for the occurrence of SAFT in rich hydrocarbon flames.